Sabelnikov V, Lipatnikov A, Chakraborty N, Nishiki S, Hasegawa T.

A balance equation for the mean rate of product creation in premixed turbulent flames.

***Proceedings of the Combustion Institute* (2016)**

DOI: http://dx.doi.org/10.1016/j.proci.2016.08.018

A Balance Equation for the Mean Rate of Product Creation in Premixed Turbulent Flames

Vladimir A. Sabelnikov[a], Andrei N. Lipatnikov[b], Nilanjan Chakraborty[c],

Shinnosuke Nishiki[d], Tatsuya Hasegawa[e]

[a] *ONERA - The French Aerospace Lab., F-91761 Palaiseau, France*

[b] *Department of Applied Mechanics, Chalmers University of Technology, Göteborg, 412 96, Sweden*

[c] *School of Mechanical and Systems Engineering, Newcastle University, Newcastle-Upon-Tyne NE1 7RU, UK*

[d] *Department of Mechanical Engineering, Kagoshima University, Kagoshima 890-0065, Japan*

[e] *EcoTopia Science Institute, Nagoya University, Nagoya 464-8603, Japan*

Abstract

Transport equations for reaction rate W and its Favre-averaged value $\tilde{W}$ are derived from first principle in the case of premixed turbulent combustion. The assumptions made for derivation hold for unity Lewis number premixed flames at least in the flamelet regime of turbulent burning. Analysis of the latter equation shows that it involves two dominant terms, but the difference between them vanishes if reaction zones retain the structure of the zone in the unperturbed laminar flame. However, in such a case, turbulent burning velocity cannot grow with time during interaction of an initially laminar flame with a turbulent flow. Therefore, the analysis indicates a vital role played by local perturbations of reaction zone structure in premixed turbulent combustion. The dominance of these two terms and the important role played by the difference between them are confirmed by analyzing three DNS databases associated with both the corrugated flamelets and thin reaction zones regimes of premixed turbulent burning. Moreover, the DNS data show that perturbations of local displacement speed due to perturbations of local flamelet structure are also of paramount importance for modeling transport of flame surface density even in weakly turbulent flows. Finally, by simulating curved and/or strained

laminar premixed flames and integrating the transport equation for W across the flames, the integral is shown to depend linearly on the stretch rate even in highly perturbed flames, with results obtained from variously stretched flames being close to each other. Based on this finding, the difference between the two dominant terms in the transport equation for the mean rate $\tilde{W}$ is hypothesized to depend linearly on the stretch rate conditioned to the reaction zone. Application of this hypothesis to the DNS data associated with the corrugated flamelets combustion regime yields encouraging results, thus, confirming a crucial role played by local perturbations of reaction zone structure even in weakly turbulent flames.

Keywords: premixed turbulent combustion, mean reaction rate, flame stretch, DNS, modeling

1. Introduction

As reviewed elsewhere [1-8], a variety of models have been proposed to evaluate Favre-averaged reaction rate $\bar{\rho}\tilde{W} \equiv \overline{\rho W}$ in premixed turbulent flames in the case of a single-step chemistry. Some of these models invoke an extra balance equation for (i) the mean scalar dissipation rate (SDR) $\bar{\rho}\tilde{\chi} \equiv \overline{2\rho D \nabla c'' \cdot \nabla c''}$ [7, 9], (ii) mean Flame Surface Density (FSD) $\overline{\Sigma}$ [10-13], or (iii) variance $\overline{\rho c''^2}$ used to close presumed Probability Density Function (PDF) $P(c, \tilde{c}, \overline{\rho c''^2}/\bar{\rho})$ [14, 15]. Here, ρ is the density, c is the combustion progress variable, D is the molecular diffusivity, W is the rate of product creation, and $c'' \equiv c - \tilde{c}$. Mantel and Borghi [9] converted their mean SDR transport equation to a transport equation of $\overline{\rho W}$ by (i) utilizing the following expression $\overline{\rho W} = \bar{\rho}\tilde{\chi}/(2c_m - 1)$ derived by Bray [16] for high Damköhler number (i.e. $Da \gg 1$) flames and (ii) considering $c_m = \int_0^1 \rho W c f(c) dc / \int_0^1 \rho W f(c) dc$ to be a constant. Here, $f(c)$ is the burning mode probability density function [16]. It is worth noting, however, that the latter transport equation is a model equation, which is restricted to $Da \gg 1$ and does not include e.g. dilatation effects [7] or spatial variations of c_m, which are well pronounced even at high Da [17]. The goal of the present work is to derive and analyze an exact transport of W.

In the next section, an unclosed transport equation for $\tilde{W}$ is derived and discussed. In the third

section, numerical simulations are summarized. In the fourth section, results are reported, followed by conclusions.

2. Transport Equation

2.1. Derivation

Let us assume that the state of the mixture is characterized with a single combustion progress variable c, e.g. $\rho = \rho(c)$, i.e. the flame is adiabatic, the Mach number is low, the Lewis number $Le = 1$, etc. [4]. Let us also assume that the rate W depends only on c, i.e. $W = W(c)$. Then, using the continuity

$$\frac{\partial \rho}{\partial t} + \nabla \cdot (\rho \mathbf{u}) = 0, \tag{1}$$

and c-transport

$$\rho \frac{\partial c}{\partial t} + \rho \mathbf{u} \cdot \nabla c = \nabla \cdot (\rho D \nabla c) + \rho W \tag{2}$$

equations, we arrive at

$$\begin{aligned} \frac{\partial}{\partial t}(\rho W) + \nabla \cdot (\rho \mathbf{u} W) &= \rho \frac{\partial W}{\partial t} + \rho \mathbf{u} \cdot \nabla W \\ = \frac{dW}{dc}\left[\rho \frac{\partial c}{\partial t} + \rho \mathbf{u} \cdot \nabla c\right] &= \frac{dW}{dc} \nabla \cdot (\rho D \nabla c) \\ + \rho W \frac{dW}{dc} &= \nabla \cdot \left(\rho D \frac{dW}{dc} \nabla c\right) \\ - \rho D \nabla c \cdot \nabla \left(\frac{dW}{dc}\right) &+ \rho W \frac{dW}{dc} \\ = \nabla \cdot (\rho D \nabla W) - \rho N \frac{d^2 W}{dc^2} &+ \rho W \frac{dW}{dc}, \end{aligned} \tag{3}$$

where t is time, $\mathbf{u}$ is the flow velocity vector, and $N \equiv D \nabla c \cdot \nabla c$. Equation (3) has a standard structure, i.e. unsteady and convection terms on the Left Hand Side (LHS) and diffusion and sink/source terms on the Right Hand Side (RHS). These sink/source terms change their sign within a flame, because the sign of $W'' = d^2W/dc^2$ or $W' = dW/dc$ changes with c.

Ensemble averaging of Eq. (3) yields

$$\frac{\partial}{\partial t}\left(\bar{\rho}\tilde{W}\right) + \nabla \cdot \overline{\rho \mathbf{u} W}$$
$$= \nabla \cdot \overline{\rho D \nabla W} - \overline{\rho N W''} + \overline{\rho W W'} \quad (4)$$

Equation (3) can also be filtered for LES. Equation (4) has been derived invoking a single assumption that the rate W depends solely on c if $Le = 1$ and this assumption is expected to be valid for unity Lewis number premixed flames at least in the flamelet regime of premixed turbulent burning. Such an assumption is widely used by the theory of stretched laminar flames [18, 19] and by various models of premixed turbulent burning [2-15].

2.2. Discussion

First, application of Eq. (3) to an unperturbed planar 1D laminar premixed flame, followed by integration along a normal to the flame results in

$$\int_{-\infty}^{\infty} \left(\rho N W'' - \rho W W'\right) dx = 0. \quad (5)$$

Therefore, the source/sink terms exactly balance each other after integration along a normal to an unperturbed laminar premixed flame.

Second, application of Eq. (4) to a statistically planar, 1D turbulent premixed flame yields

$$\frac{\partial}{\partial t}\left(\bar{\rho}\tilde{W}\right) + \underbrace{\frac{\partial}{\partial x}\overline{\rho u W}}_{T_1}$$
$$= \underbrace{\frac{\partial}{\partial x}\overline{\left(\rho D \frac{\partial W}{\partial x}\right)}}_{T_2} \underbrace{-\overline{\rho N W''}}_{T_3} + \underbrace{\overline{\rho W W'}}_{T_4}. \quad (6)$$

Integration of this equation along x results in

$$\rho_u \frac{\partial U_t}{\partial t} = \int_{-\infty}^{\infty} \left(\overline{\rho W W'} - \overline{\rho N W''}\right) dx. \quad (7)$$

Here, $U_t \equiv \rho_u^{-1} \int_{-\infty}^{\infty} \bar{\rho}\tilde{W} dx$ is the turbulent burning velocity. Equation (7) proves that the integrated terms T_3 and T_4 should not balance each other in order for turbulent burning velocity to develop, e.g.

starting from $U_t = S_L$ at $t = 0$. Accordingly, the sum of T_3 and T_4 should not vanish in a developing turbulent flame. In a fully-developed flame, T_3 and T_4 are unlikely to locally balance each other either. Indeed, if $(T_3 + T_4) = 0$, then, the stationary Eq. (7) reduces to $\overline{\rho u W} = \overline{\left(\rho D \frac{\partial W}{\partial x}\right)}$, but a non-trivial solution to the latter equation is hardly expected if e.g. ρD =const (this simplification is widely used in theoretical studies of premixed flames [18, 19]). As will be discussed later local imbalance between terms T_3 and T_4 is associated with perturbations of the local structure of reaction zones by turbulent stretching.

Third, in the corrugated flamelets regime associated with large Damköhler $Da = \tau_t/\tau_c$ and low Karlovitz $Ka = (\delta_L/\eta)^2$ numbers, the probability γ of finding intermediate $(0 < c < 1)$ states of the reacting mixture can be assumed to be low everywhere within the mean flame brush and the following bimodal PDF [16]

$$P(\mathbf{x}, t, c) \approx [1 - \bar{c}(\mathbf{x}, t)]\delta(c)$$
$$+\bar{c}(\mathbf{x}, t)\delta(1 - c) + \gamma(\mathbf{x}, t)P_f(\mathbf{x}, t, c) \quad (8)$$

can be invoked. Here, $\tau_t = L/u'$ and $\tau_c = D_u/S_L^2$ are turbulence and flame time scales, respectively, u' is the rms turbulent velocity, L and $\eta = LRe_t^{-3/4}$ are integral and Kolmogorov length scales, respectively, $\delta_L = D_u/S_L$ is the laminar flame thickness, $Re_t = u'L/\nu_u$ is the turbulent Reynolds number, ν_u is the kinematic viscosity of unburned gas, $\delta(1 - c)$ and $\delta(c)$ are Dirac delta functions. For brevity, dependencies of P, $\bar{c}$, γ, etc. on spatial coordinates $\mathbf{x}$ and time t will not be specified in the following. Accordingly,

$$\bar{\rho}\tilde{W} = \overline{\rho W} = \int_0^1 \rho(c)W(c)P(c)dc$$
$$= \gamma \int_0^1 \rho(c)W(c)P_f(c)dc = \gamma\rho_u W_*, \quad (9)$$

where W_* is a scale for the local rate $W(c)$. In order for the term $\bar{\rho}\tilde{W}$ to play a role in the ensemble-averaged Eq. (2), this source term should be comparable with the LHS terms, i.e. the product of γW_* should be on the order of U_t/δ_t, where δ_t is the mean flame brush thickness. The use of the same

W_* and Eq. (8) in order to estimate various terms in Eq. (6) shows that T_3 and T_4 are on the order of $\gamma\rho_u W_*^2 \propto \gamma^{-1}\rho_u(U_t/\delta_t)^2 \gg \rho_u(U_t/\delta_t)^2$, whereas other terms are on the order of $\rho_u(U_t/\delta_t)^2$ or less. Therefore, in the corrugated flamelets regime, T_3 and T_4 should dominate.

Fourth, in a general case, we can write

$$P(c) = \alpha\delta(c) + \beta\delta(1-c)$$
$$+\gamma_1 P_{f,1}(c) + \gamma_2 P_{f,2}(c), \tag{10}$$

where coefficients α, β, γ_1, γ_2 and functions $P_{f,1}(c)$, $P_{f,2}(c)$ are unknown, but $P_{f,1}(c > c_w) = P_{f,2}(c < c_w) = 0$, with c_w being associated with the boundary of the reaction zone, i.e. $W(c < c_w)$ can be disregarded, but the rate W is substantial at $c > c_w$. Recent experimental data reviewed elsewhere [8, 20] indicate that reaction zones are thin even in the thin reaction zones regime. In such a case, we can assume that $\gamma_2 \ll 1$ and arrive at $\tilde{W} = O(\gamma_2 W_*) = O(U_t/\delta_t)$, $T_1 = O[\rho_u(U_t/\delta_t)^2]$, $T_2 = O[\rho_u D_u U_t/\delta_t^3]$, $T_3 = O[\rho_u\gamma_2^{-1}(U_t/\delta_t)^2]$, and $T_4 = O[\rho_u\gamma_2^{-1}(U_t/\delta_t)^2]$. Therefore, we can expect that terms T_3 and T_4 dominate even in the thin reaction zones regime.

Fifth, if we come back to the corrugated flamelets regime and disregard perturbations of local flamelet structure, then, $P_f(c)$ in Eq. (8) can be modeled as follows $P_f(\varepsilon < c < 1-\varepsilon) \propto (\delta_L|\nabla c|)^{-1}$ [15, 16], where $\varepsilon \ll 1$ is sufficiently small in order for contributions of ranges of $0 < c < \varepsilon$ and $1-\varepsilon < c < 1$ to the mean terms to be negligible. Accordingly,

$$\overline{\rho W W'} - \overline{\rho N W''}$$
$$\propto \gamma \int_{\varepsilon}^{1-\varepsilon} \left(\rho W W' - \rho N W''\right) \frac{dc}{\delta_L|\nabla c|}$$
$$= \gamma \int_{\xi_1}^{\xi_2} \left(\rho W W' - \rho N W''\right) d\xi = 0 \tag{11}$$

by virtue of Eq. (5). Here, ξ is the non-dimensional spatial coordinate locally normal to a flamelet and integration is performed over a single flamelet.

However, the equality of $(T_3 + T_4) = 0$, resulting from Eq. (11), is wrong. Indeed, if $(T_3 + T_4) = 0$, then, $\partial U_t/\partial t = 0$ due to Eq. (7) and the burning velocity cannot grow even if the initial $U_t = S_L$.

Thus, an assumption that local flamelet structure perturbations can be neglected, which is equivalent to substitution of $P_f \propto (\delta_L|\nabla c|)^{-1}$ into the BML PDF given by Eq. (8), results straightforwardly in Eq. (11) and, hence, in a wrong conclusion that U_t cannot develop. The assumption appears to be wrong even in statistically stationary case, because, otherwise, Eq. (6) would involve solely transport terms, but would not involve a term that controls an increase in $\tilde{W}$ from $\tilde{W} = 0$ in unburned gas. Thus, local flamelet structure perturbations cannot be neglected, i.e. they play a vital role in premixed turbulent burning. This direct consequence of the introduced W-transport equation shows that it offers an opportunity to gain fundamental insights into the physics of turbulent flames.

At a first glance, the conclusion regarding an important role played by local flamelet structure perturbations in premixed turbulent burning could seem to be trivial. Indeed, if the effect of turbulence on premixed combustion is associated with stretching and wrinkling of flamelets (or thin reaction zones) by turbulent eddies, then, the aforementioned perturbations appear to be taken into account. However, this is not true, because many models that address the flamelet stretching and wrinkling place the focus of consideration on an increase in the flamelet surface area by turbulent stretching, but, at least in the case of sufficiently weak turbulence, neglect the flamelet structure perturbations caused by the same turbulent stretching.

For instance, FSD models [3, 4] deal with the following unclosed transport equation [10-13]

$$\frac{\partial \overline{\Sigma}}{\partial t} + \nabla \cdot \overline{\mathbf{u}\Sigma} = \overline{a_t \Sigma} - \nabla \cdot \overline{S_d \mathbf{n} \Sigma} + \overline{S_d \Sigma \nabla \cdot \mathbf{n}} \tag{12}$$

for a mean FSD $\overline{\Sigma} = \overline{|\nabla c|}$. Here, $a_t = \nabla \cdot \mathbf{u} - \mathbf{nn} : \nabla \mathbf{u}$ is the strain rate, $\mathbf{n} = -\nabla c/|\nabla c|$, and

$$S_d = \frac{1}{\rho |\nabla c|} \left[\nabla \cdot (\rho D \nabla c) + \rho W \right] \tag{13}$$

is the displacement speed. Equation (12) is exact and addresses both the increase in flamelet surface area by turbulent stretching, see the first term on the RHS, and the flamelet structure perturbations, because $\rho S_d(\mathbf{x}, t) \neq \rho_u S_L$ in a general case. However, at a first glance, Eq. (12) does not seem to

necessitate $\rho S_d(\mathbf{x},t) \neq \rho_u S_L$, but appears to be consistent with a simplification[1] of $\rho S_d(\mathbf{x},t) = \rho_u S_L$ [21]. A similar simplification of $(\overline{\rho S_d})_s = \rho_u S_L$ is widely used to close Eq. (12), as reviewed elsewhere [3, 4]. Thus, contrary to Eq. (4) derived above, the FSD Eq. (12) or, to the best of the present authors' knowledge, another model of turbulent flames does not reveal a crucial role played by flamelet structure perturbations in premixed turbulent combustion.

In the next sections, we shall illustrate certain features of Eq. (4) by processing DNS data.

3. Numerical Simulations

3.1. DNS attributes

We evaluated various terms in Eq. (4) by processing three DNS databases computed by Rutland and Cant [22], by Nishiki et al. [23, 24] in Nagoya University, and by Chakraborty et al. [25, 26] in Newcastle University. In the following, these three studies will be called RC, Na, and Ne DNS, respectively. Because the DNS data were discussed in detail elsewhere [22-26] and were already used in a number of investigations, see [27-35], [17,35,36-43], [44-48] for the RC, Na, or Ne DNS, respectively, we will restrict ourselves to a brief summary of the simulations.

In all three cases, unsteady 3D balance equations for mass, momentum, energy, and mass fraction of the deficient reactant were numerically solved. The ideal gas state equation was used. Combustion chemistry was reduced to a single reaction. The Lewis and Prandtl numbers were equal to 1.0 and 0.7, respectively. Other flame characteristics are reported in Table 1, where $Da_{th} = LS_L/(u'\delta_{th})$, $Ka_{th} = (u'/S_L)^{3/2}(L/\delta_{th})^{-1/2}$, $\delta_{th} = (T_b - T_u)/\max|dT/dx|$ is the thermal laminar flame thickness, and $\sigma = \rho_u/\rho_b$ is the density ratio. The RC and Na DNSs address the corrugated flamelets regime, whereas the Ne DNS data are associated with the thin reaction zones regime [1].

Rectangular computational domains (8×4×4 mm, $36\delta_{th} \times 45\delta_{th} \times 45\delta_{th}$, and $36.2\delta_{th} \times 24.1\delta_{th} \times 24.1\delta_{th}$ in the Na, RC, and Ne DNS, respectively) were resolved using uniform Cartesian meshes of

[1] Later, we will show that the use of such a simplification can result in $\overline{\Sigma}(\bar{c}=1) \neq 0$ if $\overline{\Sigma}(\bar{c}=0) = 0$.

Table 1: Flame characteristics

Case	u'/S_L	L/δ_{th}	σ	Re_t	Da_{th}	Ka_{th}
RC	1.4	9.6	3.3	57	6.8	0.54
Na-H	0.9	15.9	7.5	96	18.0	0.21
Na-M	1.0	18.0	5.0	96	17.8	0.24
Na-L	1.3	21.8	2.5	96	17.3	0.30
Ne-B	6.3	1.4	5.5	24	0.23	13.0
Ne-C	7.5	2.5	5.5	48	0.33	13.0
Ne-D	9.0	4.3	5.5	100	0.48	13.0
Ne-E	11.3	3.75	5.5	110	0.33	19.5

512×128×128, 261×128×128, and 345×230×230 points, respectively. In all cases, the mean flow velocity was parallel to the x-axes and normal to the mean flame brush, with the periodic boundary conditions being set at the transverse sides.

In all cases, homogeneous isotropic turbulence was used to initialize velocity fluctuations and a single planar laminar flame was embedded into the computational domain at $t = 0$. In the RC and Ne DNSs, turbulence decayed with time and the mean inlet velocity $U = S_L$ was constant. Averaging was performed over transverse planes at $t/\tau_t = 4$ (RC flame), 2 (Ne flame D), 3 (Ne flames C and E), and 4.34 (Ne flame B). In the Na DNS, homogeneous isotropic turbulence was generated in a separate box, was injected into the computational domain at $x = 0$, and decayed along the direction x. Averaging was performed over transverse yz-planes and over time interval on the order of 10 ms (about 200 snapshots) during that both $U_t(t)$ and mean flame brush thickness $\delta_t(t)$ oscillated around statistically steady values [42].

These earlier DNSs did not aim at studying Eq. (4), which is introduced here. Accordingly, the used meshes may not be sufficiently fine to properly resolve spatial variations in WW' and NW''. Therefore, in the present paper, the DNS data are analyzed to gain a qualitative insight into the behavior and relative magnitudes of various terms in Eq. (4), whereas target-directed DNS with a very fine mesh is

necessary to investigate these terms quantitatively.

3.2. Simulations of perturbed laminar flames

To gain an insight into a link between Eq. (4) and local perturbations of reaction zone, we also simulated stretched laminar flames by numerically integrating the following unsteady 1D balance equations

$$\begin{aligned}&\frac{\partial}{\partial t}(\varrho\Phi)+\varrho g\Phi+\frac{1}{r^k}\frac{\partial}{\partial r}\left(r^k\varrho v\Phi\right)\\&=\frac{1}{r^k}\ \frac{\partial}{\partial r}\left[r^k\varrho^{1-m}d_\phi\frac{\partial\Phi}{\partial r}\right]+\varrho S_\phi,\end{aligned}\tag{14}$$

as discussed in detail elsewhere [49]. Here, $\Phi=\{1,\ g,\ c\}$, $d_\phi=\{0,\ D_u,\ D_u\}$, $S_\phi=\{0,\ -g^2+J^2/\varrho,\varrho W\}$, $\varrho=\rho/\rho_u=1/[1+(\sigma-1)c]$ is the normalized density, g is rate of strain, $k=\{0,1,2\}$ for planar, cylindrical, and spherical flames, respectively ($g=0$ if $k=2$), m is a power exponent of the temperature dependence of $D=D_u/\varrho^m$.

The boundary conditions were set as follows

$$\begin{aligned}&v(0,t)=\frac{\partial c}{\partial r}(0,t)=\frac{\partial g}{\partial r}(0,t)=0,\\&\frac{\partial c}{\partial r}(r_m,t)=0,\quad g(r_m,t)=J.\end{aligned}\tag{15}$$

Here, r_m corresponds to the outlet boundary of the computational domain and J is an input parameter required to vary the strain rate. The initial conditions described a small pocket of combustion products.

The flame stretch rate was evaluated as follows

$$\dot{s}=g+\frac{k}{R_f}\frac{dR_f}{dt},\tag{16}$$

with the flame coordinate R_f being obtained from a constraint of $c[r=R_f(t),t]=c_*$, where $c_*=c_m$ is associated with the peak $W(c)$. Such a method of defining flame surface is widely used in theoretical [18, 19] and numerical [50] studies of laminar flames. Because the laminar flame thickness is small and almost constant in expanding flames, computed results are weakly sensitive to the choice of c_*.

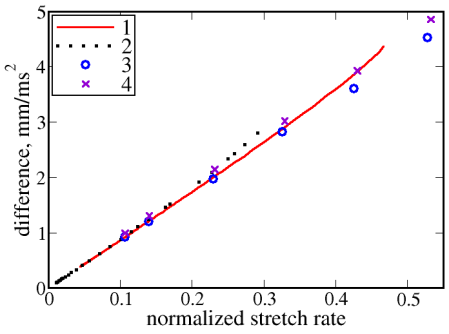

Figure 1: The LHS of Eq. (17) vs. normalized stretch rate $\tau_c \dot{s}$. Simulations were performed with σ, m, and $W(c)$ used in case H of Na DNS. 1 - expanding spherical flame ($k = 2$, $J = 0$), 2 - expanding cylindrical flame ($k = 1$, $J = 0$), 3 - steady strained cylindrical flame ($k = 1$, various J), 4 - steady strained planar flame ($k = 0$, various J).

Typical results of such simulations are reported in Fig. 1, which supports the simplest linear fit

$$\frac{1}{R_f^k} \int_0^\infty \left(\rho W W' - \rho N W'' \right) r^k dr = \rho_u V \dot{s} \tag{17}$$

for various types and strengths of flame perturbations. The dimensional coefficient V can be called "Markstein velocity" via an analogy with Markstein lengths used to characterize response of a laminar flame speed to a weak stretch rate.

4. DNS Results and Discussion

Various terms in Eq. (6) are shown in Figs. 2 and 3 in cases associated with the corrugated flamelets and thin reaction zones regimes, respectively. Due to averaging over reaction zones, the term T_3 (or T_4) assumes positive (or negative) sign within the flame brush, contrary to the instantaneous predecessor term in Eq. (3) or (14), which changes its sign following the sign of W'' (or W'). As the probability of finding burning fluid is smaller than finding unburned or burned gas, the signs of W'' and W' towards the burned gas side (i.e. $0.8 < c < 1$) ultimately determine the sign of T_3 and T_4, because W'' and W' remain negligible on the unburned gas side ($0 < c < 0.5$). In all cases, terms T_3 and T_4 dominate in line with the above discussion. Moreover, $|T_3|$ differs from $|T_4|$, with the difference magnitude, see dotted lines, being much smaller than $|T_3|$ or $|T_4|$, but comparable with $|T_1|$ or $|T_2|$. The unsteady term

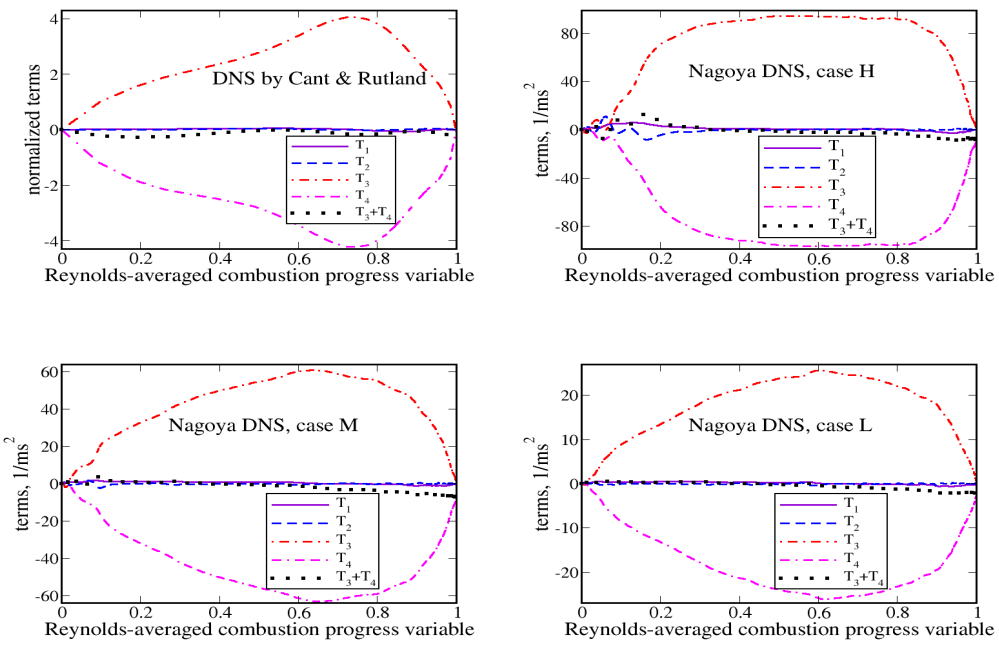

Figure 2: Various terms in Eq. (6) obtained from flames associated with the corrugated flamelets regime.

vanishes under conditions of the Na DNS and is small in other five cases.

The fact that (T_3+T_4) does not vanish, but plays a substantial role highlights flamelet perturbations, as discussed in Sect. 2.2. An important role played by the perturbations even in weakly turbulent flames is supported in Fig. 4, which compares dependencies of $\overline{\rho u W}$ on $\bar{c}$, extracted from the DNS and obtained by numerically integrating the following equation

$$\frac{\partial}{\partial x}\overline{\rho u W} = \frac{\partial}{\partial x}\overline{\left(\rho D \frac{\partial W}{\partial x}\right)} + \frac{V}{S_L}\bar{\rho}\tilde{W}\langle \dot{s} | c_{w,1} < c < c_{w,2}\rangle. \tag{18}$$

Here, V was evaluated by simulating the counterpart perturbed laminar flames, as discussed in Sect. 3.2, while all other terms on the RHS were extracted from the DNS. This equation can be obtained if (i) $\rho N W''$ and $\rho W W'$ are averaged invoking the PDF given by Eq. (8) with $P_f \propto (\delta_L |\nabla c|)^{-1}$, (ii) the probability γ is modeled as follows $\gamma = \bar{\rho}\tilde{W}\delta_L/S_L$ by applying the same PDFs to averaging W, and (iii) Eq. (17) is used to integrate $\rho W W' - \rho N W''$ over flamelets. Because W, $\rho N W''$, and $\rho W W'$ vanish beyond the reaction zone, the local stretch rate $\dot{s}$ is conditioned to c-values associated with the

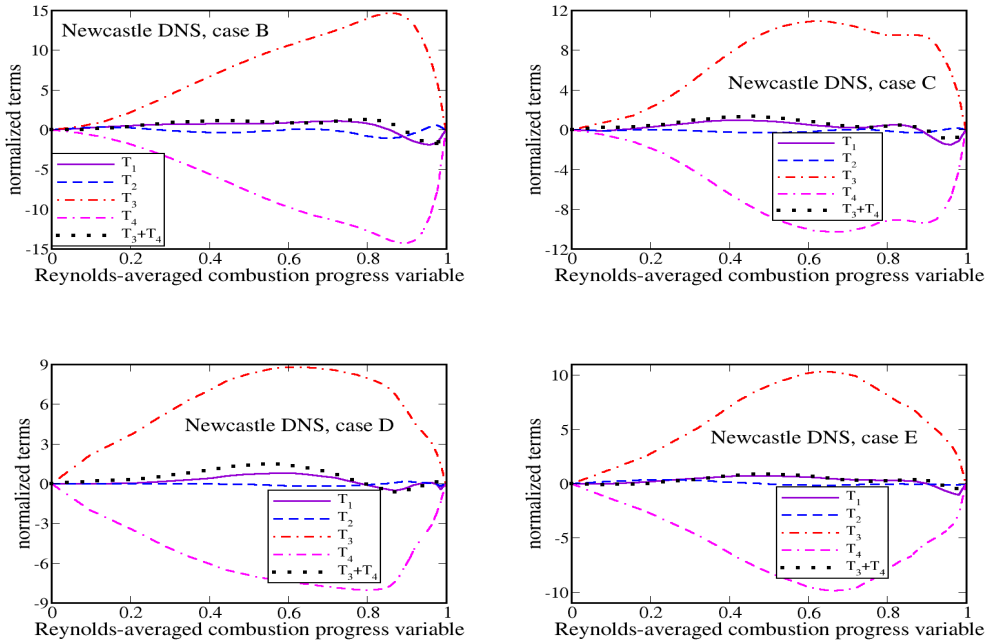

Figure 3: Various terms in Eq. (6) obtained from flames associated with the thin reaction zones regime.

reaction zone, and weak dependencies of the computed results on the choices of $c_{w,1}$ and $c_{w,2}$ have been ensured.

Because (i) importance of local perturbations of reaction zones is recognized for highly turbulent flames and (ii) the model Eq. (18) relies on the flamelet paradigm, we will restrict ourselves to assessment of this model using weakly turbulent Na DNS data, which pertain [17] to the corrugated flamelets regime. Moreover, these DNS cases deal with statistically stationary flames, and, thus, the suggested joint closure relation for $(T_3 + T_4)$ can be tested using a well-resolved quantity such as $\overline{\rho u W}$, thereby, circumventing the aforementioned problem of eventually insufficiently fine numerical resolution of spatial variations in $\rho N W''$ and $\rho W W'$ in the case of the Na DNS. For the thin reaction zones regime [1], the problem of closing $(T_3 + T_4)$ requires further analysis.

Figure 4 shows that Eq. (18) predicts $\overline{\rho u W}(\bar{c})$ in a reasonably satisfactory manner, thus, indicating an important role played by local flamelet structure perturbations even in weakly turbulent flames. If $\tilde{W} = (\overline{\rho u W} - \overline{\rho u'' W''})/(\bar{\rho}\tilde{u})$ is evaluated using the model $\overline{\rho u W}$, with other terms being extracted from

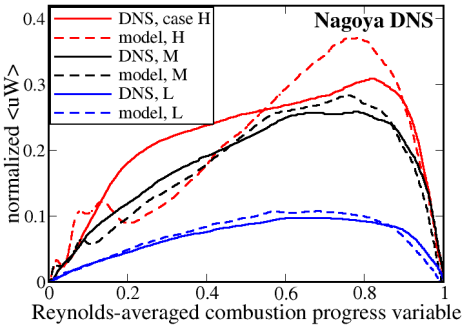

Figure 4: Normalized flux $\overline{\rho u W} D_u/(\rho_u S_L^3)$ vs. $\bar{c}$. Solid and dashed lines show results extracted from the DNS and obtained by integrating Eq. (18), respectively. $c_{w,1} = 0.55$ and $c_{w,2} = 0.99$.

the Na DNS, the spatial integration of the model $\tilde{W}$ yields $U_t = 1.09$, 0.94, and 0.75 m/s for Na flames H, M, and L, respectively, and these values are close to $U_t = 1.15$, 1.02, and 0.75 m/s, respectively, extracted straightforwardly from the DNS.

An important role played by flamelet structure perturbations is consistent with the FSD Eq. (12). To show this consistency, we evaluated $\overline{u\Sigma}$ by numerically integrating Eq. (12), with all terms on the RHS being extracted from the Na DNS. Subsequently, $\overline{\Sigma} = (\overline{u\Sigma} - \overline{u'\Sigma'})/\bar{u}$ was calculated using the DNS data on $\overline{u'\Sigma'}$ and $\bar{u}$. Results obtained by substituting S_d computed using Eq. (13) into Eq. (12) agree very well with $\overline{\Sigma}$ extracted straightforwardly from the DNS, cf. solid and dotted lines in Fig. 5, thus, validating the simulations.[2] However, if the correct Eq. (13) is substituted with an approximation of $S_d(\mathbf{x}, t) = \rho_u S_L/\rho$ when extracting the two last terms on the RHS of Eq. (12) from the same DNS, the mean FSD is substantially overestimated, see dashed lines. In particular, $\overline{\Sigma}$ does not vanish at $\bar{c} = 1$ due to the use of this approximation. Moreover, the burning velocity $S_L \int_0^{\Lambda_x} \overline{|\nabla c|} dx$ is significantly (about 50 %) overestimated if S_d is assumed to be equal to $\rho_u S_L/\rho$. This test shows that the approximation is wrong, i.e. flamelet structure perturbations significantly affect FSD transport even in weakly turbulent

[2]The fact that these DNS cases are well resolved to analyze the FSD transport is also supported by small magnitudes of residuals obtained by extracting each term of Eq. (12) from the DNS, as discussed in [51], where the relation between S_d and S_L is also assessed straightforwardly.

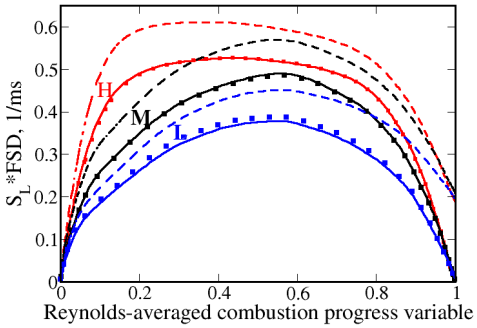

Figure 5: Mean FSD multiplied with the laminar flame speed, computed in Na DNS cases H, M, and L. Dotted lines show $S_L\overline{|\nabla c|}$ extracted from the DNS data. Solid lines show $S_L\overline{|\nabla c|}$ obtained by integrating Eq. (12), with all other terms in this equation, including S_d, being extracted from the DNS data. Dashed lines show $S_L\overline{|\nabla c|}$ obtained by integrating Eq. (12), with $S_d(\mathbf{x},t) = \rho_u S_L/\rho$ and all other terms being extracted from the DNS data.

premixed flames, in line with the above discussion.

The fact that terms T_3 and T_4 dominate in Eq. (6), with $(T_3 + T_4)$ playing a substantial role, is a challenge for closing this transport equation, because both T_3 and T_4 should be modeled with a high precision in order to predict (T_3+T_4). A similar problem arises for the closure of the transport equation for the mean scalar dissipation rate $\tilde{\chi}$ at high Reynolds numbers, but models that deal with the latter equation are successfully developed, as reviewed elsewhere [7]. Moreover, a solution could consist of studying $(T_3 + T_4)$ instead of modeling each term separately.

Figure 4 indicates that Eq. (18) is a reasonable first step to development of such a joint closure in the corrugated flamelets regime ($Ka < 1$). Difference between the DNS and model results could be attributed to inability of simple problems addressed in Sect. 3.2 to represent variety of unsteady local burning structures that exist in a premixed turbulent flame [52]. Such effects are more pronounced at $Ka > 1$ and substantial difference between DNS data and model prediction has been found for Ne-database. The difference can also be attributed to numerical resolution of these DNS cases, because a mesh sufficiently fine to resolve terms in Eq. (2) could be too coarse to resolve rapidly varying terms in Eq. (3).

Furthermore, Eq. (18) and Fig. 4 explain why $(T_3 + T_4)$ changes its sign from positive to negative when $\bar{c}$ is increased, see dotted lines in Fig. 3. The point is that positive (negative) stretch rates $\langle \dot{s} | c_{w,1} < c < c_{w,2} \rangle$ statistically dominate at the leading (trailing) part of a premixed turbulent flame brush, at least under conditions of the present DNS.

5. Conclusions

Transport equations for instantaneous reaction rate and its mean value have been derived for premixed mode of burning under the assumption which is valid at least for the flamelet regime of combustion. The latter equation reveals a vital role played by local perturbations of reaction zone structure even in weakly turbulent flames.

Acknowledgments

VS gratefully acknowledges the financial support by ONERA. AL gratefully acknowledges the financial support by CERC and Chalmers Transport Area of Advance. NC gratefully acknowledges the financial support provided by EPSRC, UK.

References

[1] N. Peters, Turbulent Combustion, Cambridge University Press, Cambridge, 2000.

[2] A. N. Lipatnikov, J. Chomiak, Prog. Energy Combust. Sci. 28 (2002) 1–74.

[3] D. Veynante, L. Vervisch, Prog. Energy Combust. Sci. 28 (2002) 193–266.

[4] T. Poinsot, D. Veynante, Theoretical and Numerical Combustion, second ed., Edwards, Philadelphia, 2005.

[5] A. N. Lipatnikov, J. Chomiak, Prog. Energy Combust. Sci. 31 (2005) 1–73.

[6] R. W. Bilger, S. B. Pope, K. N. C. Bray, J. F. Driscoll, Proc. Combust. Inst. 30 (2005) 21–42.

[7] N. Chakraborty, M. Champion, A. Mura, N. Swaminathan, in: N. Swaminathan, K. N. C. Bray (Eds.), Turbulent Premixed Flames, Cambridge University Press, Cambridge, 2011, 76–102.

[8] A. Lipatnikov, Fundamentals of Premixed Turbulent Combustion, CRC Press, Boca Raton, Florida, 2012.

[9] T. Mantel, R. Borghi, Combust. Flame 96 (1994) 443–457.

[10] S. B. Pope, Int. J. Eng. Sci. 26 (1988) 445–469.

[11] S. Candel, T. Poinsot, Combust. Sci. Technol. 170 (1990) 1–15.

[12] A. Trouvé, T. Poinsot, J. Fluid Mech. 278 (1994) 1–31.

[13] L. Vervisch, E. Bidaux, K. N. C. Bray, W. Kollmann, Phys. Fluids 7 (1995) 2496–2503.

[14] N. Peters, J. Non-Equil. Thermodyn. 7 (1982) 25–38.

[15] K. N. C. Bray, M. Champion, P. A. Libby, N. Swaminathan, Combust. Flame 146 (2006) 665–673.

[16] K. N. C. Bray, Proc. Combust. Inst. 17 (1979) 223–233.

[17] A. N. Lipatnikov, S. Nishiki, T. Hasegawa, Combust. Theory Modelling 19 (2015) 309-328.

[18] P. Clavin, Prog. Energy Combust. Sci. 11 (1985) 1–59.

[19] M. Matalon, Annu. Rev. Fluid Mech. 39 (2007) 163–191.

[20] J. F. Driscoll Prog. Energy Combust. Sci. 34 (2008) 91–134.

[21] V. L. Zimont, Combust. Flame 162 (2015) 874–875.

[22] C. J. Rutland, R. S. Cant, in: Proc. of 1994 Summer Program, Centre for Turbulence Research, Stanford University/NASA Ames, Stanford, CA, 1994, 75–94 (1994).

[23] S. Nishiki, T. Hasegawa, R. Borghi, R. Himeno, Proc. Combust. Inst. 29 (2002) 2017–2022.

[24] S. Nishiki, T. Hasegawa, R. Borghi, R. Himeno, Combust. Theory Modelling 10 (2006) 39–55.

[25] N. Chakraborty, G. Hartung, M. Katragadda, C. F. Kaminski, Combust. Flame 158 (2011) 1372–1390.

[26] N. Chakraborty, E. R. Hawkes, Phys. Fluids 23 (2011) 065113.

[27] D. Veynante, A. Trouvé, K. N. C. Bray, T. Mantel, J. Fluid Mech. 332 (1997) 263–293.

[28] N. Swaminathan, R. W. Bilger, G. R. Ruetsch, Combust. Sci. Technol. 128 (1997) 73–97.

[29] S. Tullis, R. S. Cant, Proc. Combust. Inst. 29 (2002) 2097–2105.

[30] N. Chakraborty, N. Swaminathan, Phys. Fluids 19 (2007) 045103.

[31] N. Chakraborty, J. W. Rogerson, N. Swaminathan, Phys Fluids 20 (2008) 045106.

[32] N. Chakraborty, M. Katragadda, R. S. Cant, Flow Turbul. Combust. 87 (2011) 205–235.

[33] K. N. C. Bray, M. Champion, P. A. Libby, N. Swaminathan, Combust Flame 158 (2011) 2017–2022.

[34] N. Chakraborty, A. N. Lipatnikov, J. Combust. 2011 (2011) 628208.

[35] N. Chakraborty, A. N. Lipatnikov, Proc. Combust. Inst. 34 (2013) 133-1345.

[36] Y. H. Im, K. Y. Huh, S. Nishiki, T. Hasegawa, Combust. Flame 137 (2004) 478–488.

[37] A. Mura, K. Tsuboi, T. Hasegawa, Combust. Theory Modelling 12 (2008) 671–698.

[38] A. Mura, V. Robin, M. Champion, T. Hasegawa, Flow Turbul. Combust. 82 (2009) 339–358.

[39] V. Robin, A. Mura, M. Champion, T. Hasegawa, Combust. Sci. Technol. 182 (2010) 449–464.

[40] V. Robin, A. Mura, M. Champion, J. Fluid Mech. 689 (2011) 149–182.

[41] A. N. Lipatnikov, S. Nishiki, T. Hasegawa, Phys. Fluids 26 (2014) 105104.

[42] A. N. Lipatnikov, J. Chomiak, V. A. Sabelnikov, S. Nishiki, T. Hasegawa, Proc. Combust. Inst. 35 (2015) 1401–1408.

[43] A. N. Lipatnikov, V. A. Sabelnikov, S. Nishiki, T. Hasegawa, N. Chakraborty, Flow Turbul. Combust. 94 (2015) 513–526.

[44] N. Chakraborty, H. Kolla, R. Sankaran, E. R. Hawkes, J. H. Chen, N. Swaminathan, Proc. Combust. Inst. 34 (2013) 1151–1162.

[45] L. Wang, N. Chakraborty, J. Zhang, Proc. Combust. Inst. 34 (2013) 1401–1409.

[46] N. Chakraborty, R. S. Cant, Proc. Combust. Inst. 34 (2013) 1347–1356.

[47] Y. Gao, N. Chakraborty, M. Klein, European J. Mech., Fluids-B 52 (2015) 97–108.

[48] M. Klein, C. Kasten, Y. Gao, N. Chakraborty, Comput. Fluids 122 (2015) 1–11.

[49] A. N. Lipatnikov, J. Chomiak, Combust. Sci. Technol. 137 (1998) 277–298.

[50] G. K. Giannakopoulos, A. Gatzoulis, C. E. Frouzakis, M. Matalon, A. G. Tomboulides, Combust. Flame 162 (2015) 1249–1264.

[51] A. N. Lipatnikov, V. A. Sabelnikov, S. Nishiki, T. Hasegawa, Combust. Theory Modelling, submitted.

[52] A. Amato, M. Day, R. K. Cheng, J. Bell, D. Dasgupta, T. Lieuwen, Combust. Flame 162 (2015) 4553–4565.

Figure Captions

Fig. 1. The LHS of Eq. (17) vs. normalized stretch rate $\tau_c \dot{s}$. Simulations were performed with σ, m, and $W(c)$ used in case H of Na DNS. 1 - expanding spherical flame ($k = 2$, $J = 0$), 2 - expanding cylindrical flame ($k = 1$, $J = 0$), 3 - steady strained cylindrical flame ($k = 1$, various J), 4 - steady strained planar flame ($k = 0$, various J).

Fig. 2. Various terms in Eq. (6) obtained from flames associated with the corrugated flamelets regime.

Fig. 3. Various terms in Eq. (6) obtained from flames associated with the thin reaction zones regime.

Fig. 4. Normalized flux $\overline{\rho u W} D_u/(\rho_u S_L^3)$ vs. $\tilde{c}$. Solid and dashed lines show results extracted from the DNS and obtained by integrating Eq. (18), respectively. $c_{w,1} = 0.55$ and $c_{w,2} = 0.99$.

Fig. 5. Mean FSD multiplied with the laminar flame speed, computed in Na DNS cases H, M, and L. Dotted lines show $S_L\overline{|\nabla c|}$ extracted from the DNS data. Solid lines show $S_L\overline{|\nabla c|}$ obtained by integrating Eq. (12), with all other terms in this equation, including S_d, being extracted from the DNS data. Dashed lines show $S_L\overline{|\nabla c|}$ obtained by integrating Eq. (12), with $S_d(\mathbf{x}, t) = \rho_u S_L/\rho$ and all other terms being extracted from the DNS data.